

EFFECT OF IMPINGEMENT GAP Z ON CONVECTIVE HEAT TRANSFER COEFFICIENT H**T. Onah¹, Festus L. Tor² and V.I. Henry³**¹Department of Mechanical Engineering, Enugu State University of Science and Technology (ESUT), Enugu, Nigeria²Department of Mechanical Engineering, Rivers State Polytechnic, Bori, Rivers, Nigeria³Department of Mechanical Engineering, Institute of Management and Technology (I.M.T), Enugu, Nigeria

ABSTRACT: *Experimental studies were carried out in order to evaluate the coefficient of convective heat transfer, h , an impingement air cooling method was designed for this target. Studies were carried out to determine the Convective Heat Transfer Coefficient, h , under multiple jets of impinging cold air on a target heated flat plate. Tests were run with air-distribution plates with hole diameters, d , of 1.5mm, 2.0mm, 2.5mm and 3.0mm. The target plate is a carbon-steel flat plate of 6mm thickness, instrumented with a total of three Chromel-Alumel K-type thermocouples. The plate is electrically heated using a variable supply current input. Test were run at various cooling air flow rate G , between $1.0\text{kg/m}^3, \text{sec}$ to $3.0\text{kg/m}^3, \text{sec}$. Distribution plate-to-target plate distance $Z(\text{mm})$, was varied between 100mm to 200mm. Heat input to the target plate Q Watt, was varied to give a heat flux rate between 10 to 100 watts. Results obtained were reduced and analyzed by evaluating for the dependence of h on the impingement jet diameter, Jet Reynolds Number, and the coolant mass flow rate G . Based on the results obtained, considerations were done on the effect of impingement gap Z on convective heat transfer coefficient $h, \text{w/m}^2, ^\circ\text{C}$.*

KEYWORDS: Reynold's Number, Nusselt Number, Prandtl Number, Impingement, Cooling, Heat transfer Coefficient

INTRODUCTION

Gas turbine combustors are also cooled by impinging air jets and there is increasing industrial interest to perfect the application for the cooling of combustor wall because it promises superior effectiveness over the conventional methods such as convective film and effusion cooling.

The necessity for more effective combustor wall cooling arises from the desire to obtain higher operating temperature in the gas turbine cycle for increased work per unit of mass throughput as well as better efficiency. This will lead to lighter engines and higher capacity turbines. Unfortunately, the practical limit to cycle temperature is fixed by the material of the combustor.

Many investigators have worked on impingement heat transfer. Earlier workers were more concerned with studies related to the use for heating and drying as applied in the paper and glass industries. Later workers have included other applications such as turbine blade cooling and combustor wall cooling. Some investigators worked with single rows of round and slot jets and some with multiple jet arrays.

In comparing previous work of the authors with the present work, two significant problems were encountered. Firstly, some workers had defined a heat transfer coefficient in terms of a

temperature difference between the impingement jet outlet and the target plate whereas other workers had used a temperature difference between the coolant supply temperature and the target plate. In the present work, the significance of these differences is assessed. Secondly, many other workers had used impingement geometries with significant cross flow in the impingement gap. The significance of the cross flow influences in the present work is assessed by investigating spatial temperature distributions on the impingement plate.

Due to complexity of impinging jet structures in actual arrays, researchers have systematically studied the effects of geometrical parameters on heat transfer characteristics of impinging jets. Dano, Bertrand, et-al^[1] researched on the effects of nozzle geometry on the flow characteristics and the heat transfer performance. San and lai ^[2] studied the effect of jet-to-jet impingement spacing on heat transfer in staggered arrays. Cheong and Ireland ^[3] experimentally measured local heat transfer coefficient under an impinged jet with low nozzle-to-plate, z/d spacing. Several others have studied the effect of cross flow on jet structure and heat transfer including Florsguetz^[4], Kercher and Tabakoff^[5]. Both Florschuets, and Kercher and Tabakoff developed correlations to predict the effects of cross flow on jet impingement heat transfer for inline and staggered arrays which are still used today in jet impingement research. Bailey and Bunker^[6] studied the effect of sparse and dense arrays for large number of jets. Herbert and Ekkad^[7], investigated the effect of a stream wise pressure gradient for an inline array of sparse and dense configurations.

As more information on geometrical parameters and their effect on impinging jets became available, others studied ways of increasing the jet effectiveness through target surface modification. Surface geometries such as trip strips, protrusions or dimples can significantly alter the jet structure and potentially provide enhanced heat transfer. Ekkad and Kontrovitz^[8] used a dimpled target surface.

This concept proved inadequate in heat transfer enhancement and actually showed a drop in performance. Another concept employed in many internal cooling configuration is trip strips. Small strip placed on the surface break down boundary layers, increase local turbulence levels, and enhance heat transfer. The use of trip strips was studied in detail by Han et al ^[9] for internal channel flow, and later by Herbert and Ekkad^[10] in jet impingement configurations.

Andrews, Hussain and Ojobor S.N^[11], obtained full coverage impingement Heat Transfer, the influence of impingement jet size and correlated their result as $h=460*(z/d)^{-0.15} * G^{0.8}$.

However, Hollworth and Berry ^[12] obtained a test rig with single sided air exit so that there was always an influence of cross flow. Secondly, the method of calculating the heat transfer coefficient using a long-mean of the temperature differences between the impingement plate and the plenum chamber air temperature was studied. This was an attempt to use a coolant temperature close to a jet outlet temperature. Hollworth and Berry also recognized this problem and they used a coolant temperature which was the average of the plenum temperature and jet outlet temperature. Thereafter, many other workers have used the plenum chamber temperature as the coolant. As the temperature differences between the coolant and the impingement plate varies with the coolant flow rate, the present method of evaluating h could give a slightly different value for y than using the plenum chamber temperature. This value of y is a function of z/d

In this present work - impingement of air cooling on a hot plate of varied flow rate of air, was studied on a hot target plate. The influence of temperature difference and quality of heat input

were considered for values of h , these however, were correlated with Reynolds number, Nusselt number, Prandtl number and coolant flow per unit surface area to show influence with h values.

MATERIALS AND METHODS

Design of Rig

In order to evaluate the coefficient of convective heat transfer, h , an impingement air cooling method was designed for this target.

The design is based on segment of components parts and assembly. The plenum has three chambers; the first is distribution plate chamber of circular cylinder of 250mm high by 300mm in diameter with fixed curved 40mm pipe that connects the pipe of 40mm diameter to blower. This chamber also has fixed pressure gauge and thermometer at the end. In between the iron pipes is an orifice meter connected to its plate of diameter 20mm to measure flow rate of air.

The second chamber plate is also 250mm high by 300mm in diameter. The third segment is the spacer called impingement gap (Z_1 to Z_4) that varied from 100mm high to 300mm in diameter, 150mm high and 300mm in diameter, 200mm and 250mm with same diameter. All the chambers are of 2mm thickness and made of mild steel sheet.

However each of these segments is joined by two adjustable bolt clips with aid of alien – key for different impingement gap test. This gaps Z_x is replaced with heater plate via distribution chamber at each test.

The target plate is supplied with heat by electrically insulated heater and on top of the plate is fixed three K-type thermocouples for measuring mean temperature for each test.

Other important components are four circular impingement plates of 150mm diameter, each drilled with 1.5mm, 2.0mm, 2.5mm and 3.0mm respectively, with 81 number holes in each.

Instrumentations

The calculation of convective impingement heat transfer coefficient of air and other materials involves the use of some instruments to acquire some vital data needed for the calculation. Some of these instruments used are:-

Thermocouples

Analogue K-type thermocouples were used. The range is -323K to 1573K with tolerance of $\pm 0.75\%$. K-Type is described as 3.24 x 150mm metal sheath 100cm compensating wire. This gives us the average mean temperature used in calculation of temperature difference. The K-type (Chromel–Alumel) is the most commonly general purpose thermocouple.

Thermometer

An analogue thermometer was used. This mercury thermometer of 0°C to 100°C was used to measure air temperature. Air is first blown into the plenum and its temperature was measured.

Ammeter/Voltmeter:

A multi-purpose digital clamp meter with operating features of AC current 0.1A to 1000A, AC voltage 1V to 750V and DC voltage 1V to 1000V was used with the help of variable voltmeter. As the voltage was varied with variable voltmeter, the corresponding current was automatically obtained by digital clamp meter. The product of these two quantities gave the heat input to the system used for calculations.

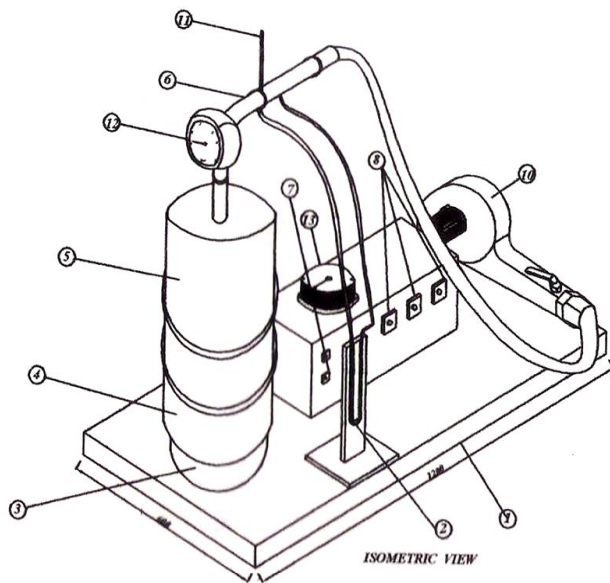
Orifice Meter

An orifice meter was used to measure pressure drops along the pipes. It was fixed on the base wood and connected to the pipe of 40mm diameter. Also connected in-between the orifice is the orifice plate of diameter 20mm inside the 40mm diameter pipe with angle of 60° vena-contracta. The pressure drop is thus measured by difference in height of water in the orifice meter with calibrated meter rule.

Pressure gauge

This was used to measure the pressure of air. This plus atmospheric pressure gives absolute pressure used in the calculation. Its calibration ranges from -1bar to 5bars

Experimental Procedure



PART LIST		
NO	DESCRIPTION	MATERIAL
1	TABLE	WOOD
2	ORIFICE METER	STOCK
3	HEATER	STAINLESS STEEL
4	SPACERS	MILD STEEL
5	RIG	MILD STEEL
6	PIPE	CAST IRON
7	VOLTMETER	STOCK
8	THERMOCOUPLES	STOCK
9	AMETER	STOCK
10	BLOWER	STOCK
11	THERMOMETER	STOCK
12	PRESSURE GAUGE	STOCK
13	VARIAC	STOCK

Fig 1 set up rig for experimentation in laboratory

Experiments were made at several air mass flow rates via orifice plate to target plate.

The procedures are as listed below:-

1. The air supply to the plenum as well as the heater was turned on.

2. The initial values of temperature and pressure of the air were read and recorded. The values of the tip temperatures of the thermocouples T_1 , T_2 & T_3 were also read and recorded.
3. The values of current and voltage were read from the ammeter and voltmeter, to obtain the quantity of heat input Q
4. Values of the pressure drop (Δh), were all recorded using the orifice meter.
5. The thermocouple readings were monitored until a near steady state – isothermal condition is achieved i.e. T_1, T_2, T_3 are within 10% of each other, and later ($T_{mean} - T_{air}$) $\geq 12^\circ\text{K}$ were obtained (by adjusting the power input to the hot plate).
6. Thereafter, final reading for that particular flow rate of air say $\frac{1}{4}$ flow rate of air was taken.
7. The experiment was repeated with a higher flow-rate of air, say $\frac{1}{2}$, $\frac{3}{4}$ and full flow.
8. After each flow rate of air the spacer (impingement gap) Z was changed and the procedures repeated as above.

EXPERIMENTAL RESULTS

The results of the experiment are shown in tables below.

Table 1 - $\frac{1}{4}$ flow rate of air @ 1.5mm impingement plate with $Z_1 = 100\text{mm}$ spacer.

S/N	T_{air}	P_{air}	A (amp)	V (volts)	Q (watt)	T1	T2	T3	T_m	$T_m - T_{air}$	Δh (cm)
1	35	0.5	0.5	1.7	8.5	160	162	162	161.3	126.3	4.4
2	35	0.5	0.7	25	17.5	180	188	188	185.3	150.3	4.4
3	35	0.5	0.9	28	25.2	200	201	205	202	167	4.4
4	35	0.5	1.1	36	39.6	225	225	225	225	190.0	4.4
5	35	0.5	1.3	50	65.0	230	230	230	230	195	4.4
6	35	0.5	1.5	56	84.0	225	225	225	225	2200	4.4
7	35	0.5	1.7	66	112.2	270	270	270	270	235.0	4.4
8	35	0.5	1.9	70	133	297	297	297	297	262.0	4.4

Table 2 - $\frac{1}{2}$ flow rate of air @ 2.0mm impingement plate with $Z_1 = 100\text{mm}$ spacer

S/N	T_{air}	P_{air}	A(amp)	V (volts)	Q (watt)	T1	T2	T3	T_m	$T_m - T_{air}$	$\Delta h(\text{cm})$
1	36	0.6	0.5	16	8.0	152	152	159	154.3	118.3	6.4
2	36	0.6	0.7	25	17.5	170	176	175	172	136.0	6.4
3	36	0.6	0.9	28	25.2	182	182	182	182	146.0	6.4
4	36	0.6	1.1	38	41.8	196	197	199	197	161.0	6.4
5	36	0.6	1.3	40	52.0	200	200	200	200	164.0	6.4
6	36	0.6	1.5	55	82.5	223	223	227	224.3	188.3	6.4
7	36	0.6	1.7	60	102.0	232	232	232	232	196.0	6.4

Table 3 -¾ flow rate air @ 2.5mm impingement plate with Z₁ = 100mm spacer.

S/N	T _{air}	P _{air}	A (amp)	V (volts)	Q (watt)	T1	T2	T3	T _m	T _m -T _{air}	Δh (cm)
1	37	0.7	0.5	15	7.5	130	134	136	133.3	96.3	7.2
2	37	0.7	0.7	25	175	153	155	157	155	118.0	7.2
3	37	0.7	0.9	30	270	170	172	176	172.7	135.7	7.2
4	37	0.7	1.1	36	39.6	191	193	195	193	156.0	7.2
5	37	0.7	1.3	42	54.6	213	215	217	215	178.0	7.2
6	37	0.7	1.7	57	76.5	232	234	236	234	197.0	7.2
7	37	0.7	1.7	57	96.9	248	249	250	249	212.0	7.2
8	37	0.7	1.9	68	129.2	260	260	260	260	223.6	7.2

Table 4 -Full flow rate of air @ 3.0mm impingement plate with Z₁ = 100mm spacer.

S/N	T _{air}	P _{air}	A(amp)	V (volts)	Q (watt)	T1	T2	T3	T _m	T _m -T _{air}	Δh (cm)
1	38	0.8	0.5	16	8.0	128	132	135	131.7	93.7	10.5
2	38	0.8	0.7	22	11.0	143	144	146	144.3	106.3	10.5
3	38	0.8	0.9	28	25.2	148	149	150	149.0	111.0	10.5
4	38	0.8	1.1	35	38.5	161	164	168	164.3	126.3	10.5
5	38	0.8	1.3	38	49.4	176	177	178	177.2	139.2	10.5
6	38	0.8	1.5	45	67.5	189	190	191	190	152.0	10.5
7	38	0.8	1.7	55	93.5	207	209	210	208.6	170.6	10.5
8	38	0.8	1.9	60	114.0	221	223	226	223.3	195.3	10.5

ANALYSIS OF RESULTS

Pipe Diameters and Number of Holes

- 1) Orifice pipe diameter = 40mm
- 2) Orifice plate diameter = 20mm
- 3) Impingement plate diameter = 150mm
- 4) Hot target plate diameter = 200mm
- 5) Number of holes, n = 81

Data Reductions

$$\text{Impingement plate area} = \dot{A} = \frac{\pi D^2}{4} = \frac{\pi(0.150)^2}{4} = 0.01767m^2 \quad (1)$$

Total mass flow rate

$$\dot{m} = \check{U} \rho_{air} A^* \quad (2)$$

$$A^* = \frac{\pi D^2}{4} = \frac{\pi (0.040)^2}{4} = 0.001257 m^2$$

Where \check{U} = velocity of orifice meter

A^* = orifice pipe sectional area

$$\check{U} = \sqrt{\frac{2\Delta P}{Cd \left(\frac{A1}{A2}\right)^2 - 1} \rho_{air}} \quad (3)$$

$$\check{U} = Cd \sqrt{\frac{2\Delta P}{\rho_{air}}} \quad (4)$$

Where Cd = coefficient of air flow from orifice plate $\cong 0.70$

$$\therefore \check{U} = 0.70 \sqrt{\frac{2\Delta P}{\rho_{air}}} \quad (5)$$

$$\text{Thus } m = \check{U} \rho_{air} (0.001257) \quad (6)$$

Where $(0.001257)m^2$ = area of orifice plate as calculated.

Data values: K = thermal conductivity for air = 0.0023567 J/m, sec, k

μ = dynamic viscosity = 1.817 x 10⁻⁵ kg/m, sec.

$$G = \frac{\dot{m}}{A'} = \frac{\dot{m}}{0.01767} \quad (7)$$

\acute{A} = Area of impingement plate calculated

G = Coolant air flow per unit surface area of the impingement plate kg/s,m²

$$Nu = \frac{hD}{K} \quad (8)$$

$$Pr = \frac{\mu C_p}{K} = 0.8828 \quad (9)$$

Where K = 0.0023567 J/sec, m, k

μ = 1.817 x 10⁻⁵ kg/m,sec (based on hole diameter)

$$Nu = \frac{hD}{0.0023567} \quad (10)$$

$$Q = h * A^* * \Delta T \quad (11)$$

$$A^* = \pi \frac{(0.20)^2}{4} = 0.0314m^2$$

$$\text{Thus, } Q = 0.0314h * \Delta T \quad (12)$$

A* = area of hot target plate = 200mm

$$\text{Thus, } Q = 0.0314 * h * (t_m - t_{air})$$

$$h = \frac{Q}{0.0314(t_m - t_{air})} \quad (13)$$

$$Nu = \frac{hD}{0.0023567} = 424.33 * h * D \quad (14)$$

$$Re = \frac{\rho_{air} VD}{\mu} \quad (15)$$

Where V = velocity through the impingement hole

Based on Jet velocity; A = jet hole area

$$\frac{\dot{m}}{n} = \rho VA \quad (16)$$

Where n = number of holes = 81

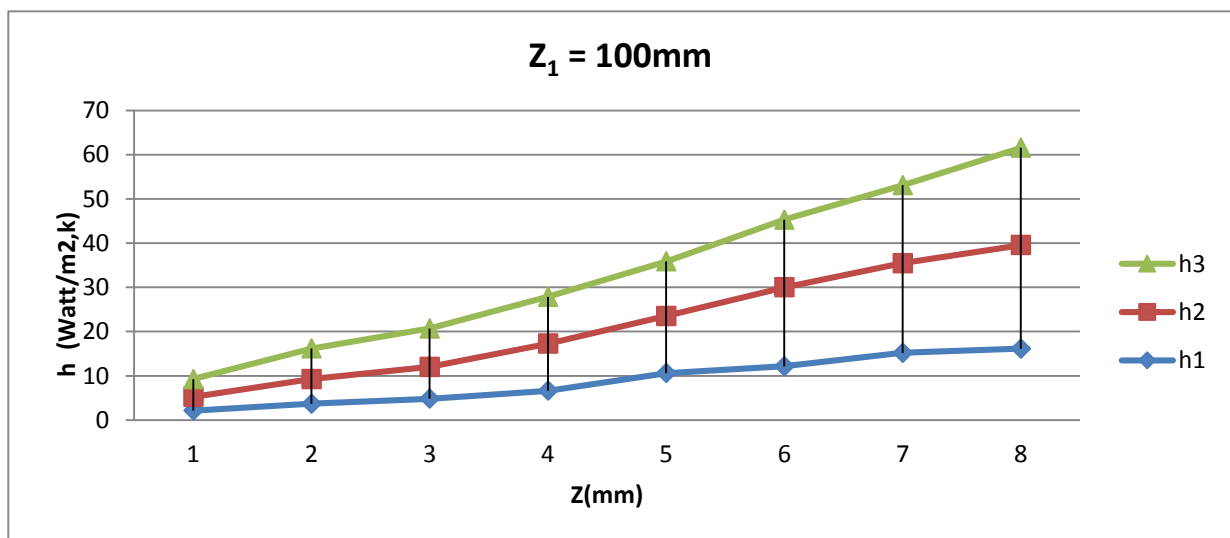
$$\mu = 1.817 * 10^{-5} \text{ kg /m, sec}$$

$$\therefore Re = 86.47 \frac{m}{D} \quad (17)$$

**EFFECT OF IMPIINGMENT GAP (Z) ON THE CONVECTIVE COEFFICIENT (H) for
Z₁ = 100mm**

Table 5: of Impingement Gap Z on the convective coefficient h for $Z_1 = 100\text{mm}$

S/No	$Z_1 = 100\text{mm}$		
	h1 (w/m ² , k)	h2(w/m ² , k)	h3(w/m ² , k)
	G = 1.92, $\Phi = 1.5\text{mm}$	G = 3.9, $\Phi = 2\text{mm}$	G = 2.54, $\Phi = 2.5\text{mm}$
1	2.14	3.09	4.020
2	3.7	5.57	6.890
3	4.8	7.21	8.700
4	6.63	10.64	10.590
5	10.61	12.93	12.320
6	12.15	17.86	15.290
7	15.19	20.28	17.620
8	16.15	22.03	23.390



h3 @ G = 2.54 kg/m², s ; Φ 2.5 mm, z = 200

h2 @ G = 2.39 kg/m², s ; Φ 2.0 mm, z = 150

h1 @ G = 1.92 kg/m², s ; Φ 1.5 mm, z = 100

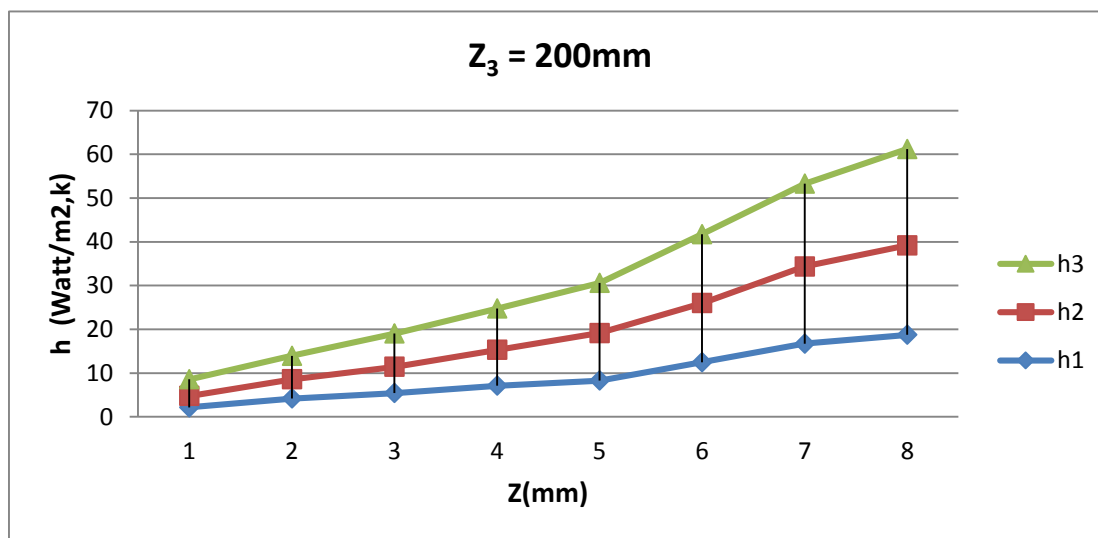
Fig 1: Plot of Convective Coefficient H versus Impingement Gap Z_1

Fig 2: Plot of Convective Coefficient H versus Impingement Gap Z_2

6.0: EFFECT OF IMPIINGMENT GAP (Z) ON THE CONVECTIVE COEFFICIENT (H) for $Z_3 = 200\text{mm}$

Table 7: of Impingement Gap Z on the convective coefficient h for $Z_3 = 200\text{mm}$

$Z_3 = 200\text{ mm}$		
h1(w/m ² , k)	h2(w/m ² , k)	h3(w/m ² , k)
G = 1.92, $\Phi = 1.5\text{mm}$	G = 3.9, $\Phi = 2\text{mm}$	G = 2.54, $\Phi = 2.5\text{mm}$
2.19	2.58	3.81
4.18	4.41	5.38
5.42	6.02	7.6
7.1	8.19	9.46
8.27	10.89	11.42
12.49	13.51	15.76
16.74	17.62	18.92
18.74	20.44	22.04



h3 @ G = 2.54 kg/m², s ; Φ 2.5 mm, z = 200

h2 @ G = 2.39 kg/m², s ; Φ 2.0 mm, z = 150

h1 @ G = 1.92 kg/m², s ; Φ 1.5 mm, z = 100

Fig 3: Plot of Convective Coefficient H versus Impingement Gap Z_3

DISCUSSION OF RESULTS

Effect of Impingement Gap z on convective heat transfer coefficient h:

Figures 1, 2 and 3 of Tables 5, 6 and 7 Graphs depict that at the same mass flow rate G and impingement hole diameter d , the impingement gaps of 100mm, 150mm and 200mm produced nearly equal convective cooling: For instant, figure 1 of plot with $z = 100\text{mm}$ gives a h value of $60\text{w/m}^2\text{ }^\circ\text{C}$. The same value of $h = 60\text{ w/m}^2\text{ }^\circ\text{C}$ is obtained at figure 2 for $z = 150\text{mm}$ and figure 3 for $z = 200\text{mm}$ (Graphs 2 and 3)

REFERENCES

- Andrews, G.E., Hussain, C.I., and Ojobor, S.N. "Full Coverage Impingement Heat Transfer. I. Chem. E., Symposium Series No 86, 1985 and Text Book on Impingement Heat Transfer: 2008
- Bailey, J.C. and R.S. Bunker Local Heat Transfer and Flow Distribution for Impinging Jet Arrays of Dense and Sparse Extent. Proc. of the ASME Turbo Expo, June 2002, Amsterdam: Netherlands.
- Ekkad, S.V. and D.M. Kontrovitz, 'Jet Impingement Heat Transfer on Dimpled Target Surfaces', International Journal of Heat and Fluid Flow Vol. 23, 2002:22-28
- Han, J.C., J.S. Park, and C.K. Lei, "Augmented Heat Transfer in Rectangular Channels of Narrow Aspect Ratios with Rib Turbulators. "International Journal of Heat and Mass Transfer Vol. 32, 1989: 1619-1630.
- Hebert, Ryan, Srinath Ekkad, and Lujai Gao. "Impingement Heat Transfer Part II: Effect of Streamwise Pressure Gradient." Journal of Thermo Physics and Heat Transfer Vol. 18, 2004.
- Hebert, Ryan, Srinath Ekkad, and Lujai Gao. "Impingement Heat Transfer Part II: Effect of Streamwise Pressure Gradient." Journal of Thermo Physics and Heat Transfer Vol. 18, 2004.
- Hollworth, B.R. and Barry, R.D. "Heat Transfer from Array of Impinging Jets with Large Jet-to-Jet Spacing, ASME, Paper No. 78 – GT-117.
- Tabakoff, W. Clevenger, W. 'Gas Turbine Heat Transfer Augmentation by Impingement of Air Jets Having Various Configurations, ASME, Journal of Engineering for Power, Jan. 1972, pp. 51-60

Appendix: Components of the Rig

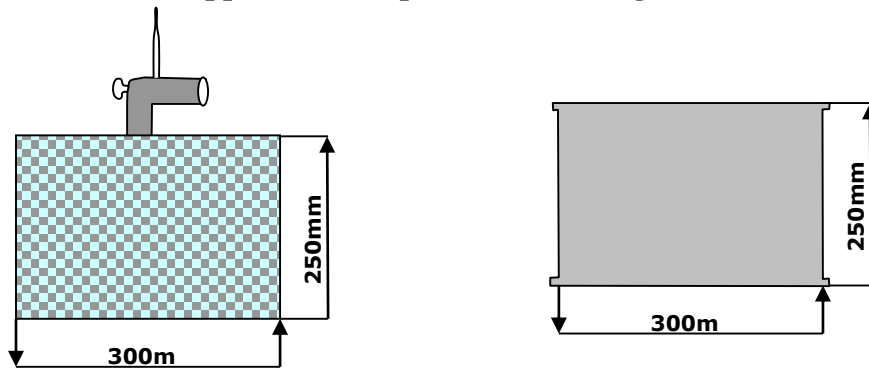


Fig 4: 1st Distribution Plenum

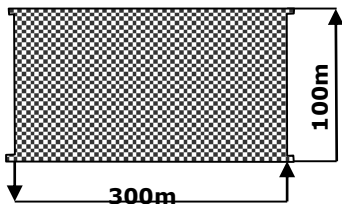


Fig 11a

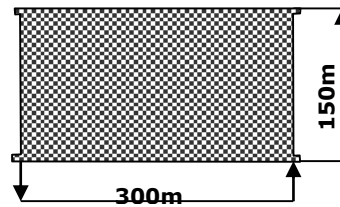


Fig 11b

Fig 5: 2nd Distribution Plenum

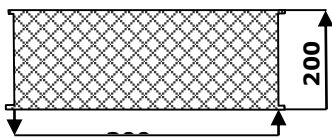


Fig 3.3.3c

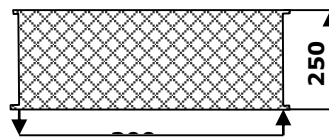


Fig 3.3.3d

Fig 6: 3rd Segment plates (impingement gaps Z_x)

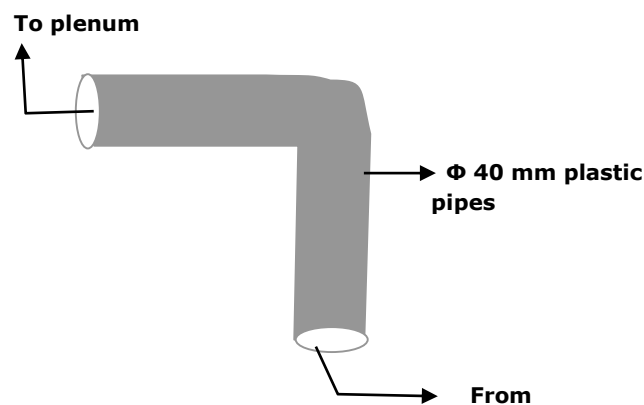


Fig6: Plastic pipe

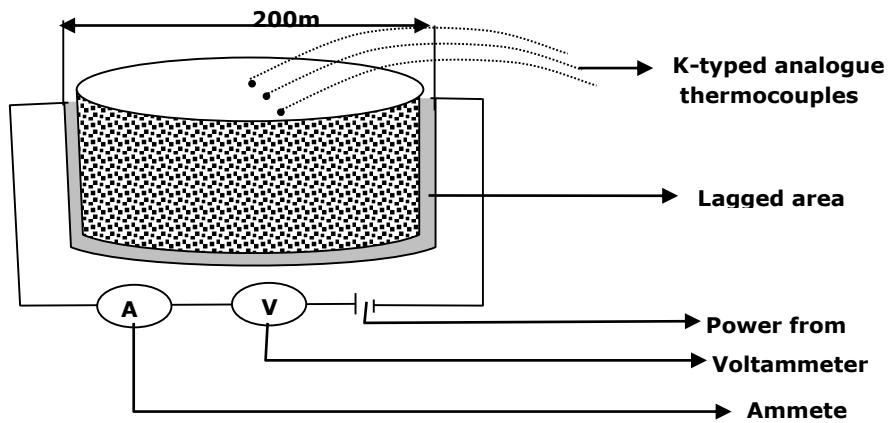


Fig7: Electric heater with thermocouples

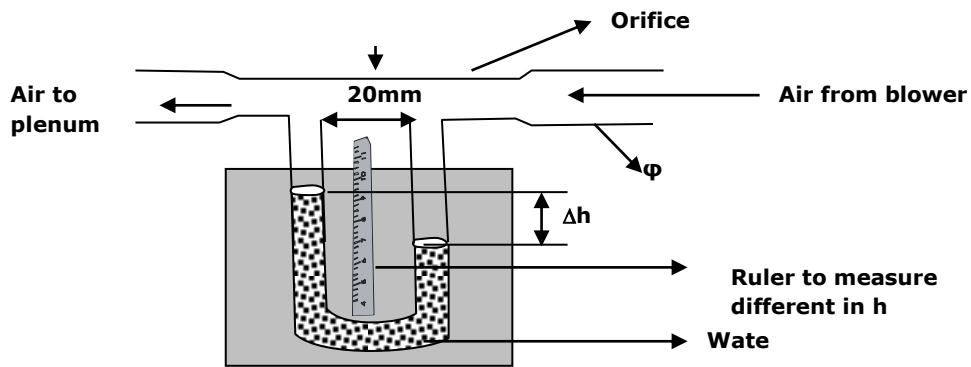


Fig 8: Orifice meter

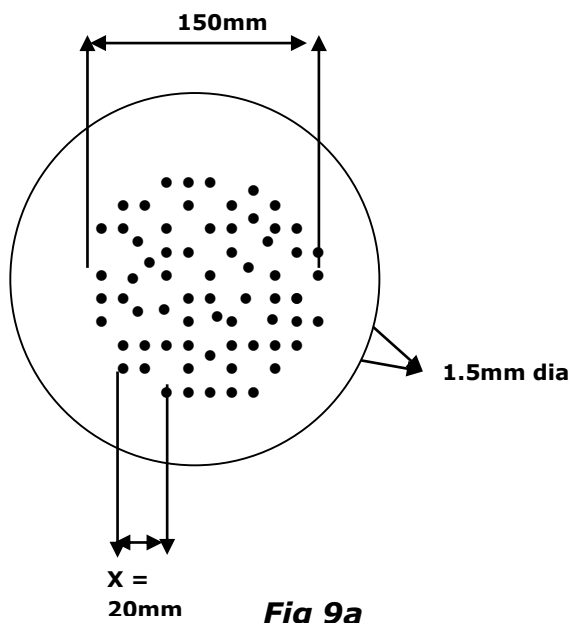


Fig 9a

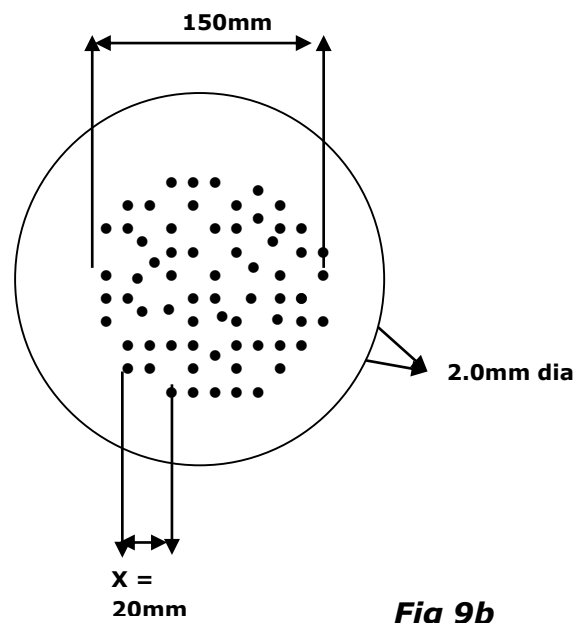


Fig 9b

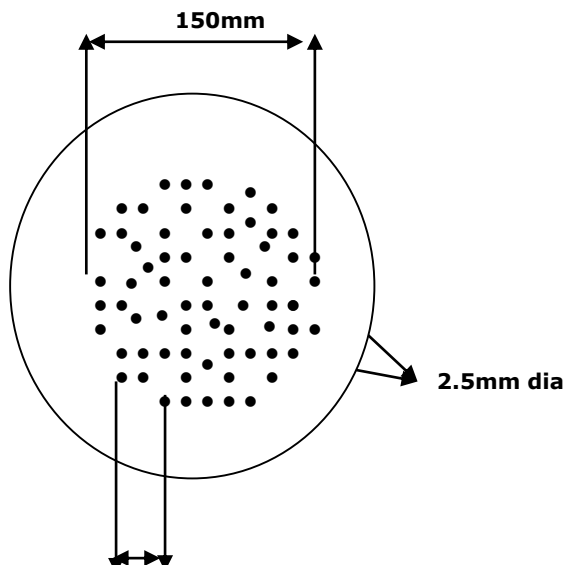


Fig 9: View of impingement plates

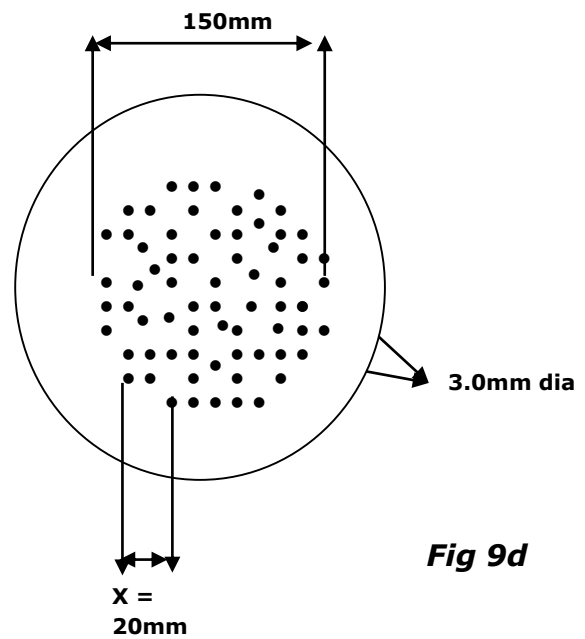


Fig 9d

The total number in each of the impingement plate is 81 holes